Magnetic Techniques for Estimating Elastic and Plastic Strains in Steels Under Cyclic Loading

E.S. Gorkunov, R.A. Savrai, and A.V. Makarov

Abstract The effect of high-cycle fatigue loading (elastic deformation) of high-carbon steel (1.03 wt% C) on the behaviour of the tangential component of the magnetic induction vector of a specimen in the residual magnetization state has been studied. It has been found that the magnetic measurement technique allows both structural changes and cracks resulting from the fatigue degradation of high-carbon pearlitic steel to be recorded. The effect of cyclic loading in the low-cycle fatigue region (plastic deformation) on the variations in the coercive force and residual magnetic induction of annealed medium-carbon steel (0.45 wt% C) for the major and minor magnetic hysteresis loops has also been studied. The sensitivity of the magnetic characteristics to both large and small plastic strains accumulated during cyclic loading has been established.

1 Introduction

In most machines and structures components operate under conditions of cyclically varying loads with regularly or irregularly alternating cycles and different levels of stresses in the cycles. The level of stresses under different conditions may correspondingly vary over a wide range and cause both elastic and plastic strains in the components. This significantly complicates the study of fatigue resistance, the prediction of durability and the determination of residual life, and it requires a vast amount of experimental data and full-scale tests. It is therefore necessary to apply methods that, along with collecting experimental data, would enable one to understand the physical background of fatigue as a phenomenon. In this connection,

E.S. Gorkunov (✉) · R.A. Savrai · A.V. Makarov
Institute of Engineering Science, RAS (Ural Branch), 34 Komsomolskaya str., 620049 Ekaterinburg, Russia
e-mail: ges@imach.uran.ru

Alexander K. Belyaev et al. (eds.), *Mechanics and Model-Based Control of Advanced Engineering Systems*, DOI 10.1007/978-3-7091-1571-8_15,

the application of nondestructive test methods, particularly magnetic ones, is very promising.

In the course of fatigue loading, repeated elastic deformation induces structural changes and accumulated damage thus affecting the magnetic properties of a specimen. To detect fatigue damage of the kind, it is promising to apply magnetic inspection of articles in the residual magnetization state with the use of highly sensitive transducers enabling one to make local measurements of stray magnetic fields, including those arising at defects [1, 2].

Among the magnetic characteristics used for evaluating the physical-mechanical properties of a material under plastic deformation, one can select coercive force and residual magnetic induction, which are affected by changes in dislocation density and the appearance of discontinuities (plastic loosening, microcracks and pores) [3, 4]. In this connection, it seems reasonable to divide changes in the magnetic characteristics and microstructure of a material under plastic deformation into three stages, namely, (1) at small strains; (2) at medium strains; (3) after large strains [4].

Thus, the aim of this work is to study the effect of cyclic loading of (1) high-carbon pearlitic steel (1.03 wt% C) under high-cycle fatigue (elastic deformation) on the behaviour of the tangential component of the magnetic induction vector for a specimen in the residual magnetization state; (2) annealed medium-carbon steel (0.45 wt% C) under low-cycle fatigue (plastic deformation) on the behaviour of coercive force and residual magnetic induction for the major and minor magnetic hysteresis loops.

2 Experimental Procedure and Material

Commercially cast high-carbon (1.03 wt% C) and medium-carbon (0.45 wt% C) steels were studied. The structure of fine-lamellar pearlite in high-carbon steel was obtained by 5 min isothermal holding of specimens (preheated for 15 min to 1,050 °C) in a salt bath at 500 °C followed by cooling in water. The specimens were then annealed in a salt bath at 650 °C for 10 min. Medium-carbon steel was annealed at 800 °C for 8 h and then cooled slowly with an oven to room temperature.

The specimens made from high-carbon pearlitic steel were cyclically loaded with controlled stress values $\Delta\sigma = 2\sigma_a = 0.65\sigma_{0.2}$ (where $\sigma_{0.2}$ is offset yield strength under static tension), the cycle asymmetry coefficient $R_\sigma = 0$ (intermittent zero-to-tension stress cycle) and a loading frequency of 10 Hz, the cycle stress variations obeying the sine law. The specimen was loaded step by step, with the numbers of loading cycles $N = 20{,}000, 60{,}000, 100{,}000, 160{,}000$. The specimens made from annealed medium-carbon steel were cyclically loaded with a controlled value of total strain $\epsilon_{tot} = 2\epsilon_a = \epsilon_{el} + \epsilon_{pl} = 0.0076$ (where ϵ_a is total strain amplitude, ϵ_{el} is the elastic part of the strain, ϵ_{pl} is the plastic part of the strain), a pulsating deformation cycle, the triangular change of the strain amplitude and a loading frequency of 0.5 Hz. The testing was conducted so that the cycle asymmetry coefficients ($R_\epsilon = \epsilon_{min}/\epsilon_{max}$, $R_\sigma = S_{min}/S_{max}$) met the condition $R_\epsilon = R_\sigma = 0$. The specimens were cyclically loaded with $N = 5$, 10, 50, 200 and 400 cycles.

Magnetic measurements of the tangential component of the magnetic induction vector B_t for high-carbon pearlitic steel were made with a flux-gate transducer by scanning the surface of a residually magnetized specimen along its axis at a velocity of 2 mm s^{-1}. The coercive force and residual magnetic induction of annealed medium-carbon steel were measured for the major magnetic hysteresis loop ($H_{max} = 60$ kA/m) and minor ones corresponding to the maximum magnetic induction of a hysteresis cycle $b_{max} = 1$, 0.4, 0.1 and 0.05 T respectively.

3 Results and Discussion

Let us consider the effect of high-cycle fatigue loading (elastic deformation) of high-carbon pearlitic steel on the variation of the tangential component of the magnetic induction vector B_t. It follows from Fig. 1 that the fatigue tests are accompanied by the appearance of nonuniformity in the distribution of the tangential component of the magnetic induction vector along the specimen length in the residual magnetization state; this is noted even at $N = 60{,}000$. After fatigue loading with $N = 100{,}000$, a noticeable increase in B_t was observed. This may be due to structural changes occurring in the pearlitic steel during fatigue loading, in particular, to the spheroidization of cementite lamellae. The spheroidization of fine cementite lamellae during cyclic tension under high-cycle fatigue conditions is due to the cooperative effect of elastic tensile stresses, microplastic strain and local heating accelerating the diffusion of iron and carbon atoms [5].

With the number of cycles $N = 160{,}000$, a clearly pronounced peak is observed in the distribution of the tangential component of the magnetic induction vector B_t (see Fig. 1). It is due to the appearance of a main fatigue crack initiated at the stress concentrator on the specimen surface (Fig. 2). Note that the width of the fatigue crack opening is less than 1 μm, and this testifies to the feasibility of the nondestructive inspection of the fatigue degradation of steels under high-cycle fatigue loading (elastic deformation).

Consider now the effect of low-cycle fatigue loading (plastic deformation) of annealed medium-carbon steel on its magnetic behaviour.

The initial annealed state is characterized by minimum values of the coercive force, see Table 1.

Under cyclic loading, the increasing structural imperfection density is accompanied by increasing values of the critical fields of interaction between domain walls and defects [6]. This results in the growth of coercive force values for both major and minor magnetic hysteresis loops (Fig. 3a, b). Note a considerable difference between the behaviour of the coercive force in strong fields and that in weak ones. For weak fields (0.1 T and lower, when the maximum hysteresis loop field $h_{max} < H_c$), the coercive force for minor magnetic hysteresis loops continuously rises during the whole deformation process, with a sharp increase observed at the early stage of

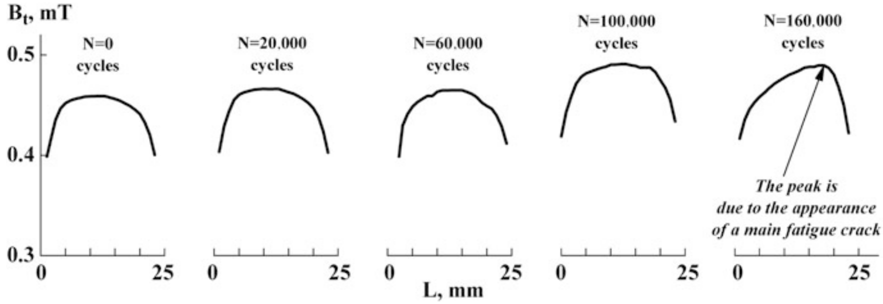

Fig. 1 Distribution of the tangential component of the magnetic induction vector B_t along the gage length of a specimen in the residual magnetization state before loading (N = 0) and after loading with a given numbers of cycles. The test results are given for the specimen side where a main fatigue crack was found

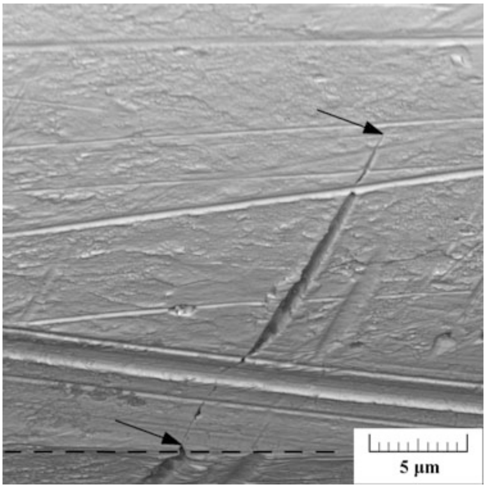

Fig. 2 An electron micrograph (SEM) of the specimen surface (after loading with the number of cycles $N = 160{,}000$). The *arrows* show a fatigue crack. The *dashed line* corresponds to the specimen edge parallel to the loading axis

Table 1 The values of coercive force (h_c, H_c) and residual magnetic induction (b_r, B_r) for medium-carbon steel in the initial annealed state (the number of cycles $N = 0$, accumulated plastic strain $\epsilon_\Sigma = 0$)

$b_{max} = 0.05\ T$		$b_{max} = 0.1\ T$		$b_{max} = 0.4\ T$		$b_{max} = 1\ T$		$H = 60$ kA/m (main loop)	
h_c, A/m	b_r, T	h_c, A/m	b_r, T	h_c, A/m	b_r, T	h_c, A/m	b_r, T	H_c, A/m	B_r, T
15.55	0.017	31.8	0.043	99.7	0.3	146.2	0.766	194.5	1.159

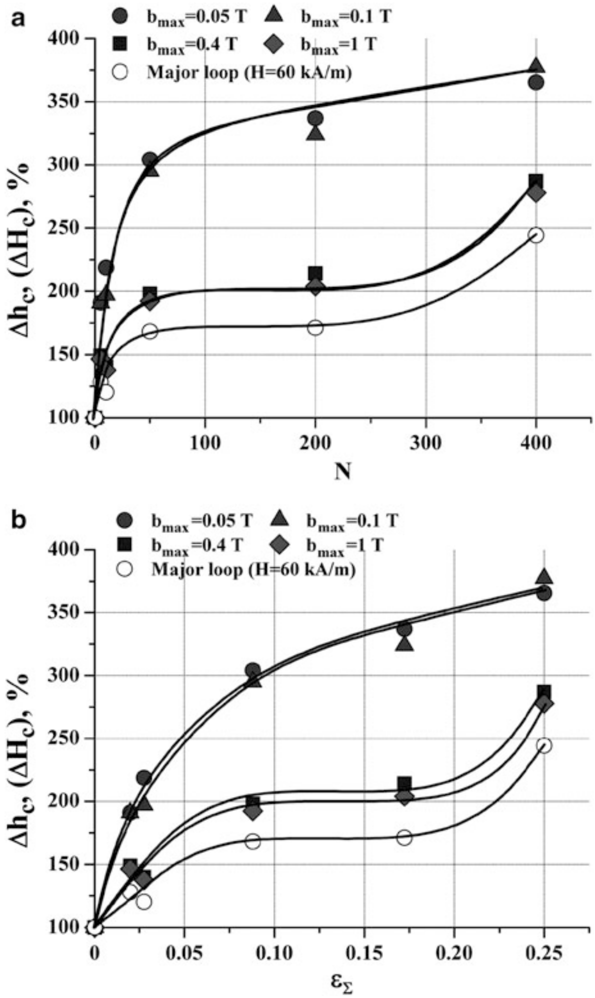

Fig. 3 Relative change in the coercive force as dependent on the number of loading cycles (**a**) and accumulated plastic strain (**b**) for medium-carbon steel specimens. Coercive force values in the initial annealed state are taken to be 100 %, see Table 1

deformation and a subsequent smoother growth at larger strains. The reason is that, in weak magnetic fields, domain walls interact mainly with single dislocations or structural imperfections having small critical fields $H_{cr} \approx h_{max}$.

Under magnetization reversal in stronger fields, one can see the stabilization of coercive force values as the accumulated plastic strain varies between 0.07–0.1 and 0.15–0.17. The stabilization may be caused by the formation of a cellular dislocation structure. In this case, domain walls interact with both individual dislocations and cell walls [6]. The further deformation is again accompanied by increasing coercive force values, and this is attributable to the appearance of microscopic pores, which grow in size and number up to fracture. Being a source of stray fields, the microscopic pores hinder magnetization reversal according to the inclusion theory [7].

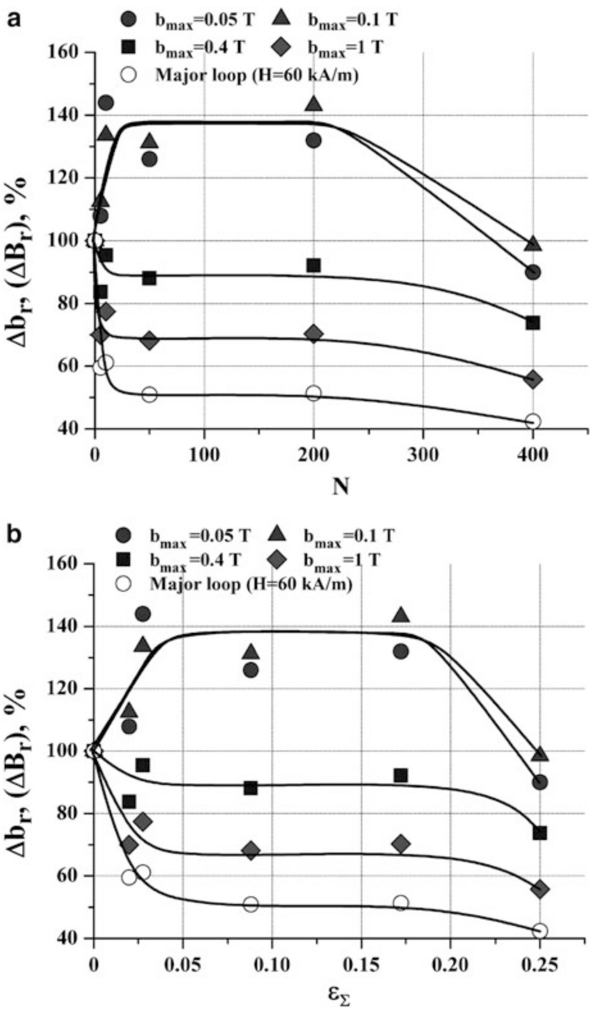

Fig. 4 Relative change in residual magnetic induction as dependent on the number of loading cycles (**a**) and accumulated plastic strain (**b**) for medium-carbon steel specimens. Residual induction values in the initial annealed state are taken to be 100 %, see Table 1

In the early stage of deformation, at a total plastic strain of 0.07–0.1 and lower, the values of residual magnetic induction decrease for the major loop and the minor loops corresponding to the maximum magnetic induction $b_{\max} = 1$ and 0.4 T, and (at a total plastic strain of 0.02–0.03 and lower) they increase for the minor loops corresponding to the maximum magnetic induction $b_{\max} = 0.1$ and 0.05 T (Fig. 4a, b).

Thus, as is the case with the coercive force, there is a difference between the variation of residual magnetic induction in week fields and that in strong ones. On the one hand, segments with large local microstresses (in particular, dislocations) are the sites where magnetization reversal centers are easily generated [7]. This contributes to a decrease in residual magnetic induction for strong fields. On the other hand, dislocation redistribution induces regions with a less imperfect structure. Magnetization in weak fields is accompanied by small domain wall displacements, which do not seem to be larger than these regions. Therefore the values of residual magnetic induction for weak fields grow up to the complete formation of a cellular dislocation structure in the whole bulk of the material. The values of residual magnetic induction stabilize thereafter up to a strain of 0.15–0.17. The further deformation is accompanied by decreasing residual magnetic induction regardless of the field magnitude, this being attributable to the appearance of microscopic pores. On macrodefects, (cracks and pores) there appear stray fields [7] directed oppositely to the magnetizing field, and this finally results in lower values of residual induction.

4 Conclusion

It has been found that the high-cycle fatigue loading (elastic deformation) of high-carbon steel specimens (1.03 wt% C) up to fatigue cracking causes an increase in the tangential component of the magnetic induction vector of a specimen in the residual magnetization state and the nonuniform distribution of the component along the specimen length. This is due to structural changes (spheroidization of cementite lamellae) occurring in high-carbon pearlitic steel under high-cycle fatigue loading. The formation of a main fatigue crack is accompanied by the appearance of a clearly pronounced peak in the distribution of the tangential component of the magnetic induction vector. The possibility of inspecting the fatigue degradation of steels under cyclic loading in the region of high-cycle fatigue has been shown.

The dependences describing the behaviour of the coercive force and residual magnetic induction for the major and minor magnetic hysteresis loops as a function of the number of loading cycles (the value of accumulated plastic strain) have been obtained for cyclically loaded specimens made from annealed medium-carbon steel (0.45 wt% C) in the low-cycle fatigue region. The dependences testify to the sensitivity of the magnetic characteristics studied to both large and small plastic strains. The possibility of using the values of magnetic parameters to inspect plastic strain accumulated during cyclic loading has been demonstrated.

Acknowledgements The work was supported by project No. 12-P-1-1027 according to RAS Presidium program No. 25.

References

1. Gorkunov, E.S., Novikov, V.F., Nichipuruk, A.P., Nassonov, V.V., Kadrov, A.V., Tatlybaeva, I.N.: Residual magnetization stability of heat-treated steel articles to the action of elastic deformations. Defektoskopiya (2), 68–76 (1991)
2. Gloria, N.B.S., Areiza, M.C.L., Miranda, I.V.J., Rebello, J.M.A.: Development of a magnetic sensor for detection and sizing of internal pipeline corrosion defects. NDT&E Int. **42**(8), 669–677 (2009)

3. Shah, M.B., Bose, M.S.C.: Magnetic NDT technique to evaluate fatigue damage. Phys. Stat. Solidi (a). **86**(1), 275–281 (1984)
4. Babich, V.K., Pirogov, V.A.: On the features of coercive force change under deformation of annealed carbon steels. Phys. Met. Metall. **28**(3), 447–453 (1969)
5. Makarov, A.V., Savrai, R.A., Schastlivtsev, V.M., Tabatchikova, T.I., Yakovleva, I.L., Egorova, L.Y.: Structural features of the behavior of a high-carbon pearlitic steel upon cyclic loading. Phys. Met. Metall. **111**(1), 95–109 (2011)
6. Vicena, F.: On the influence of dislocations on the coercive force of ferromagnetics. Czechosl. J. Phys. **5**(4), 480–499 (1955)
7. Mikheev, M.N., Gorkunov, E.S.: Magnetic Methods of Structure Analysis and Nondestructive Testing. Nauka, Moscow (1993)